

1,4-Disubstituted-[1,2,3]triazolyl-containing analogs of MT-II – design, synthesis, conformational analysis, and biological activity

Chiara Testa, Mario Scrima, Manuela Grimaldi, Anna Maria D'Ursi, Marvin Louie Servanez Dirain, Nadège Lubin-Germain, Anamika Singh, Carrie Haskell-Luevano, Michael Chorev, Paolo Rovero, and Anna Maria Papini

J. Med. Chem., **Just Accepted Manuscript** • DOI: 10.1021/jm501027w • Publication Date (Web): 27 Oct 2014

Downloaded from <http://pubs.acs.org> on October 29, 2014

Just Accepted

“Just Accepted” manuscripts have been peer-reviewed and accepted for publication. They are posted online prior to technical editing, formatting for publication and author proofing. The American Chemical Society provides “Just Accepted” as a free service to the research community to expedite the dissemination of scientific material as soon as possible after acceptance. “Just Accepted” manuscripts appear in full in PDF format accompanied by an HTML abstract. “Just Accepted” manuscripts have been fully peer reviewed, but should not be considered the official version of record. They are accessible to all readers and citable by the Digital Object Identifier (DOI®). “Just Accepted” is an optional service offered to authors. Therefore, the “Just Accepted” Web site may not include all articles that will be published in the journal. After a manuscript is technically edited and formatted, it will be removed from the “Just Accepted” Web site and published as an ASAP article. Note that technical editing may introduce minor changes to the manuscript text and/or graphics which could affect content, and all legal disclaimers and ethical guidelines that apply to the journal pertain. ACS cannot be held responsible for errors or consequences arising from the use of information contained in these “Just Accepted” manuscripts.



1
2
3
4
5 1,4-Disubstituted-[1,2,3]triazolyl-containing analogs
6
7
8
9
10 of MT-II – design, synthesis, conformational
11
12
13
14 analysis, and biological activity
15
16
17

18 *Chiara Testa,^{†,‡,¶} Mario Scrima,^{∇†} Manuela Grimaldi,[∇] Anna M. D' Ursi,[∇] Marvin L. Dirain,^{||}*

19
20
21 *Nadège Lubin-Germain,[†] Anamika Singh,^{||§} Carrie Haskell-Luevano,^{||§} Michael Chorev,^{*,⊥,¥}*

22
23 *Paolo Rovero,^{‡,¶} and Anna M. Papini.^{*,†,¶,||}*

24
25
26
27 [†] Laboratoire SOSCO & PeptLab@UCP, EA4505, University of Cergy-Pontoise, F-95031

28
29 Cergy-Pontoise CEDEX, France

30
31 [#] Department of Chemistry “Ugo Schiff”, University of Florence, I-50019 Sesto Fiorentino, Italy

32
33 [¶] Laboratory of Peptide and Protein Chemistry and Biology, University of Florence, I-50019

34
35 Sesto Fiorentino, Italy

36
37
38 [∇] Department of Pharmacy, University of Salerno, I-84084 Fisciano (Salerno), Italy

39
40
41 ^{||} Departments of Pharmacodynamics, University of Florida, Gainesville, FL 32610, USA

42
43 [§] Medicinal Chemistry, University of Minnesota, Minneapolis, MN 55455, USA

44
45
46
47 [⊥] Laboratory for Translational Research, Harvard Medical School, One Kendall Square, Building
48 600, Cambridge, MA 02139, USA

49
50
51 [¥] Department of Medicine, Brigham and Women's Hospital, 75 Francis Street, Boston, MA
52 02115, USA

53
54
55
56
57 [‡] Department NeuroFarBa, Section of Pharmaceutical and Nutraceutical Sciences, University of
58 Florence, I-50019 Sesto Fiorentino, Italy

1
2
3
4
5
6
7
8
9
10
11
12
13
14
15
16
17
18
19
20
21
22
23
24
25
26
27
28
29
30
31
32
33
34
35
36
37
38
39
40
41
42
43
44
45
46
47
48
49
50
51
52
53
54
55
56
57
58
59
60

KEYWORDS: Click Chemistry, melanocortin hormones, structure-activity-conformation-relationship.

ABSTRACT

Side chain-to-side chain cyclizations represent a strategy to select a family of bioactive conformations by reducing the entropy and enhancing the stabilization of functional ligand-induced receptor conformations. This structural manipulation contributes to increased target specificity, enhanced biological potency, improved pharmacokinetic properties, increasing functional potency, lowering metabolic susceptibility. The Cu^I-catalyzed azide-alkyne 1,3-dipolar Huisgen's cycloaddition, the prototypic click reaction, presents a promising opportunity to develop a new paradigm for an orthogonal bio-organic and intramolecular side chain-to-side chain cyclization. In fact, the proteolytic stable 1,4- or 4,1-disubstituted [1,2,3]triazolyl moiety is isosteric with the peptide bond and can function as a surrogate of the classical side chain-to-side chain lactam forming bridge. Herein we report the design, synthesis, conformational analysis, and functional biological activity of a series of i-to-i+5 1,4- and 4,1-disubstituted [1,2,3]triazole-bridged cyclopeptides derived from MT-II, the homodetic Asp⁵ to Lys¹⁰ side chain-to-side chain bridged heptapeptide, extensively studied agonist of melanocortin receptors.

INTRODUCTION

Melanocortins are a group of peptide hormones including adrenocorticotropin (ACTH) and α -, β -, and γ -melanocyte stimulating hormones (MSHs). To date, five human melanocortin receptors (MC1R-MC5R) have been characterized as belonging to group α of the rhodopsin family of G-protein coupled receptors (GPCR).^{1,2} The MCRs mediate a plethora of biological functions that

1
2
3 include sexual function,³ feeding behavior,^{4,5} pain modulation,⁶ thermoregulation, energy
4
5 homeostasis,^{7,8} cardiovascular effects, and skin pigmentation,^{9,10} making them potential drug
6
7 targets for treating pain, food intake, and body weight as well as erectile dysfunction. Therefore,
8
9 development of an expansive toolbox of structural modifications that can be used to fine tune the
10
11 predominant conformations to achieve modulation of specificity toward receptor subtypes,
12
13 physicochemical and pharmacological properties continues to be of great interest in the
14
15 development of peptide-based drugs in general and melanocortineric drugs in particular.
16
17 Recently, the growing interest in design highly selective and potent super-agonist of the human
18
19 melanocortin receptors hMC3R and hMC4R has been driven by their prospects of becoming
20
21 effective drugs for treating feeding disorders such as the respective obesity and energy
22
23 homeostasis. Structure-activity relationship studies (SAR) of α -MSH,¹¹ a post-translationally
24
25 generated tridecapeptide fragment originating from proopiomelanocortin (POMC),¹² led to the
26
27 development of MT-II, N^{α} -Ac[Nle⁴,c(Asp⁵,D-Phe⁷,Lys¹⁰)] α MSH(4-10)NH₂.^{13,14,15} This
28
29 homodetic Asp⁵ to Lys¹⁰ side chain-to-side chain bridged lactam stabilizes the pharmacophore
30
31 containing sequence His⁶-D-Phe⁷-Arg⁸-Trp⁹ in a type-II β -turn resulting in a potent long acting
32
33 non-selective super-agonist of MCRs.¹⁶ Evidently, the plethora of melanocortin-mediated
34
35 activities, the five melanocortin receptor subtypes, and the high profile of potential therapeutic
36
37 targets associated with the melanocortin system underscores the unmet need for highly selective,
38
39 pharmacokinetically diverse, and bioavailable agonists and antagonists. Intramolecular side
40
41 chain-to-side chain cyclization of linear peptides is an established approach to achieve
42
43 stabilization of specific conformations and a recognized strategy to improve resistance toward
44
45 proteolytic degradation, increasing the metabolic stability *in vitro* and *in vivo*.^{17,18} We have
46
47 previously reported a novel intramolecular i-to-i+4 side chain-to-side chain [1,2,3]triazolyl-
48
49
50
51
52
53
54
55
56
57
58
59
60

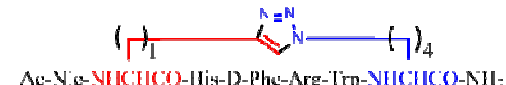
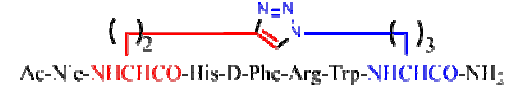
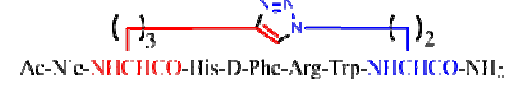
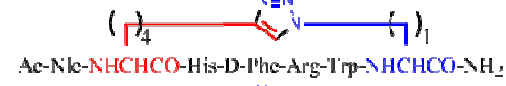
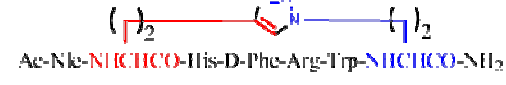
1
2
3 bridged modification that is bioisosteric to the peptide bond and employs the prototypical click
4 reaction, Cu^I-catalyzed azido-to-alkyne 1,3-dipolar cycloaddition (CuAAC).¹⁹ Importantly, the
5 CuAAC does not require synthetic schemes with elaborate orthogonal protection strategies. Our
6 studies explored the relationship between the size of the bridge containing the [1,2,3]triazolyl
7 moiety, the location of this moiety within the bridge, its orientation relative to the peptide
8 backbone, and the predominant conformations displayed by these heterodetic cyclic peptides.
9

10
11
12
13
14
15
16
17
18 In the current study we explored the potential of the i-to-i+5 side chain-to-side chain 1,4- and
19 4,1-disubstituted [1,2,3]triazolyl-containing bridges to stabilize β -turn conformations in the
20 context of the MT-II scaffold and evaluate its potential as a modulator of receptor sub-type
21 selectivity. We synthesized a series of heterodetic MT-II related cyclo-heptapeptides that varied
22 in the size of the disubstituted [1,2,3]triazolyl-containing bridge connecting C α s of residues 4
23 and 10 and in the location and orientation of the [1,2,3]triazolyl moiety within the bridge (I-X,
24 Schemes 1 and 2). The [1,2,3]triazolyl moiety was flanked on each side by 1 to 4 methylenes
25 totaling in 4 or 5 methylenes. The biological activity of all the 1,4- and 4,1-disubstituted-
26 [1,2,3]triazolyl-containing cyclopeptides (I-X, Table 2) is compared to the prototypic lactam-
27 containing peptide MT-II, as well as to the linear control precursors (I'-X', Tables 1 and 2).
28
29
30
31
32
33
34
35
36
37
38
39
40
41
42
43
44
45
46
47
48
49
50
51
52
53
54
55
56
57
58
59
60

SYNTHETIC STRATEGY

In the current study we explored the potential of the i-to-i+5 side chain-to-side chain 1,4- and 4,1-disubstituted [1,2,3]triazolyl-containing bridges to stabilize β -turn structure, which has been identified as the MT-II bioactive conformation, responsible for its protracted, non-selective and super-agonist activity. To this end we designed a series of [1,2,3]triazolyl-containing cycloheptapeptides, derived from the model lactam peptide, MT-II N^α -Ac[Nle⁴,c(Asp⁵,D-Phe⁷,Lys¹⁰)] α MSH(4-10)NH₂, that vary in the size of the bridge and the location and orientation of the [1,2,3]triazolyl moiety within this bridge (Schemes 1 and 2).

Scheme 1: Sequences of the linear precursors N^α -Ac[Nle⁴,Yaa⁵,D-Phe⁷,Xaa¹⁰] α MSH(4-10)NH₂ and of the [1,2,3]triazolyl-containing cyclo-peptides, N^α -Ac[Nle⁴,Yaa⁵(&¹),D-Phe⁷,Xaa¹⁰(&²)] α MSH(4-10)NH₂ [$\{\&^1(\text{CH}_2)_n-1,4-[1,2,3]\text{triazolyl}-(\text{CH}_2)_m\&^2\}$].^{20,*}

Linear Precursor	4,1-disubstituted 1,2,3-triazolyl cyclopeptide
I' Ac-Nle- Pru (His-D-Phe-Arg-Trp-Nle(6-N ₃))-NH ₂	I 
II' Ac-Nle- Hex(5-ynoic) -His-D-Phe-Arg-Trp-Nva(8-N ₃)-NH ₂	II 
III' Ac-Nle- Hept(6-ynoic) -His-D-Phe-Arg-Trp-hAla(7-N ₃)-NH ₂	III 
IV' Ac-Nle- Oct(7-ynoic) -His-D-Phe-Arg-Trp-Ala(3-N ₃)-NH ₂	IV 
IX' Ac-Nle- Hex(5-ynoic) -His-D-Phe-Arg-Trp-hAla(7-N ₃)-NH ₂	IX 

*All amino acids except when mentioned otherwise are of the L configuration.

Scheme 2: Sequences of the linear precursors N^{α} -Ac[Nle⁴,Xaa⁵,D-Phe⁷,Yaa¹⁰]αMSH(4-10)NH₂ and of the [1,2,3]triazolyl-containing cyclo-peptides, N^{α} -Ac[Nle⁴,Xaa⁵(&¹),D-Phe⁷,Yaa¹⁰(&²)]αMSH(4-10)NH₂ [{&¹(CH₂)_m-1,4-[1,2,3]triazolyl-(CH₂)_n&² }].*

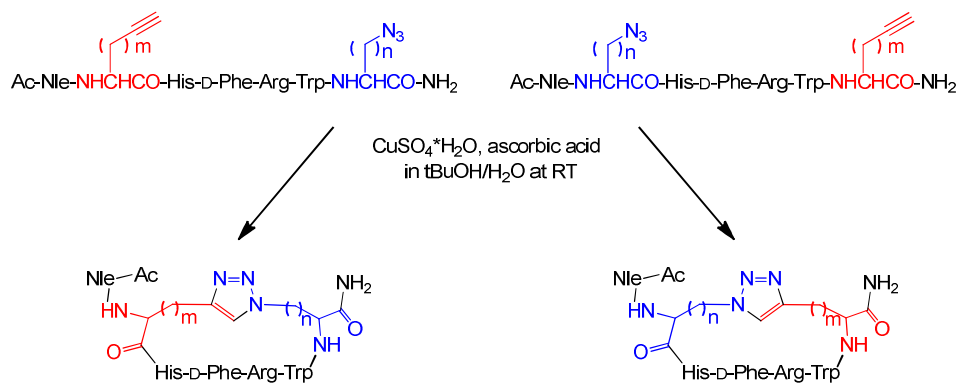
Linear Precursor		1,4-disubstituted 1,2,3-triazolyl cyclopeptide	
V'	Ac-Nle-Nle(β -N ₃)-His-D-Phe-Arg-Trp-Pra-NH ₂	V	
VI'	Ac-Nle-Nva(δ -N ₃)-His-D-Phe-Arg-Trp-Hex(γ -ynoic)-NH ₂	VI	
VII'	Ac-Nle-hAla(γ -N ₃)-His-D-Phe-Arg-Trp-Hep(δ -ynoic)-NH ₂	VII	
VIII'	Ac-Nle-Ala(β -N ₃)-His-D-Phe-Arg-Trp-Ox(γ -ynoic)-NH ₂	VIII	
X'	Ac-Nle-hAla(γ -N ₃)-His-D-Phe-Arg-Trp-Hex(δ -ynoic)-NH ₂	X	

*All amino acids except when mentioned otherwise are of the L configuration.

In this context, N^{α} -Fmoc- ω -azido- α -amino acids (**1-4**) and N^{α} -Fmoc- ω -ynoic- α -amino acids (**5-8**) with different length of the side chain were introduced in positions *i* and *i*+5 to replace Asp⁵ and Lys¹⁰ residues in the sequence of MT-II (see I'-X', Schemes 1 and 2).^{21,22} The N^{α} -Fmoc- ω -azido- α -amino acids (**1-4**) were synthesized by diazo-transfer reaction starting from the corresponding N^{α} -protected α,ω -diamino acids (see Supporting Information).²² Except for the commercially available N^{α} -Fmoc-*S*-Pra-OH (**8**) the N^{α} -Fmoc- ω -alkynyl- α -amino acids (**5-7**) were synthesized by alkylation of a Ni(II) complex of the Schiff base formed between glycine and (S)-2-(*N*-benzylpropyl)aminobenzophenone, as a chiral inducer, with alk- ω -ynyl bromides (see Supporting Information).²² Solid-phase peptide synthesis (SPPS) generated a series of linear peptide precursors (I'-X') in which Lys¹⁰ and Asp⁵ were replaced with ω -azido- and ω -yl- α -amino acid residues with side chains containing 1-4 methylenes. The stepwise solid-phase

assembly of the linear precursors I'-X', was performed following Fmoc/tBu strategy on Rink-amide type resin.²³ The chemical inertness of the ω -azido and ω -alkynyl functions toward the entire range of coupling and deprotection reactions and the various nucleophiles and electrophiles present during the multistep synthesis,^{24,25,26} saves the need for elaborate orthogonal protection schemes. The incorporation of the building blocks N^α -Fmoc-Xaa(ω -N₃)-OH and N^α -Fmoc-Yaa(ω -yl)-OH during the SPPS was found to be markedly advantageous to the post-peptide assembly side-chain modification that introduces the ω -azido and ω -ynoic functions needed for the Cu^I-catalyzed intramolecular azide-alkyne cycloaddition.^{21,22} Solution-phase intramolecular CuAAC converted the linear precursors I'-X' into the 1,4- and 4,1-disubstituted-[1,2,3]triazolyl-containing cyclopeptides (I-X), presenting different permutation in terms of the size of the [1,2,3]triazolyl-containing bridges and the orientation and position of the [1,2,3]triazolyl moiety within the bridge. Depending on the positions i or i+5 of the azido and alkynyl amino acids in the peptide sequences, we generated two classes of cyclopeptides (Schemes 1 and 2). The intramolecular CuAAC of the linear precursors (I'-X') was carried out as outlined in Scheme 3.

Scheme 3. General procedure of CuAAC of the linear precursors (I'-X').



1
2
3 The first class employed linear precursors that had ω -yl- and ω -azido- α -amino acid residues in
4 the respective positions i and $i+5$ (I'-IV' and IX') and yielded upon CuAAC the cyclopeptides
5 presenting the [1,2,3]triazolyl moiety in the 4,1-orientation (I-IV and IX). The second class
6 employed linear precursors that had ω -azido- and ω -yl- α -amino acid residues in the respective
7 positions i and $i+5$ (V'-VIII' and X') and yielded upon CuAAC the cyclopeptides presenting the
8 [1,2,3]triazolyl moiety in the 1,4-orientation (V-VIII and X). The click reaction conditions were
9 identical to those reported by us previously and used a 10-fold molar excess of $\text{CuSO}_4 \cdot 5\text{H}_2\text{O}$ and
10 ascorbic acid in $t\text{BuOH}/\text{H}_2\text{O}$ (1:2, v/v).²¹ Under these conditions, there was no formation of
11 oligomeric products resulting from intermolecular click reactions, thus suggesting formation of a
12 Cu^{I} /acetylide/azide complex that has high preference for intramolecular cyclizations. Moreover,
13 solution-phase CuAAC avoids dimerizations and macrocyclizations, which are often observed in
14 on-resin CuAAC, resulting in crude products that are easy to purify. All copper salts were
15 eliminated by solid-phase extraction of the crude material with water and elution of the
16 cyclopeptides with 10 to 30% of ACN in water. The clicked cyclopeptides were further purified
17 by RP-HPLC. The linear analog of MT-II, BE124 ($\text{Ac-Nle-Asp-His-D-Phe-Arg-Trp-Lys-NH}_2$)
18 and the its uncharged variant BE123, $\text{Ac-[Asn}^5\text{,Lys}^{10}(\text{N}^\epsilon\text{-Ac})\text{]BE124}$, were synthesized by
19 Fmoc/ $t\text{Bu}$ SPPS strategy and used as reference compounds in the biological assays (Scheme 4
20 and Table 1).
21
22
23
24
25
26
27
28
29
30
31
32
33
34
35
36
37
38
39
40
41
42
43
44

45 46 47 RESULTS AND DISCUSSION

48
49 **Biological activity.** The potency of MT-II and of the linear peptide NDP-MSH (Scheme 4),
50 the super-potent and long acting agonist,²⁷ the reference peptides BE124 and BE123 (Scheme 4),
51 and the precursors (I'-X'), as well as the [1,2,3]triazolyl-containing cyclopeptides (I-X)
52 (Schemes 1 and 2), was pharmacologically evaluated for functional potency (EC_{50}) and efficacy
53
54
55
56
57
58
59
60

1
2
3 using a reporter gene based bioassay for cAMP in HEK-293 cells stably expressing the murine
4
5 (mouse) melanocortin receptor subtypes mMC1R, mMC3R, mMC4R, and mMC5R (Tables 1-2).
6
7

8
9 **Scheme 4:** sequences of MT-II, the classical NDP-MSH, and the MT-II linear analogs – BE123
10
11 and BE124.
12

13
14 Reference Peptides

15
16
17 MT-II: Ac-Nle-c[Asp-His-D-Phe-Arg-Trp-Lys]-NH₂
18

19
20 NDP-MSH: Ac-Ser-Tyr-Ser-Nle-Glu-His-D-Phe-Arg-Trp-Gly-Lys-Pro-Val-NH₂
21

22
23 BE124: Ac-Nle-Asp-His-D-Phe-Arg-Trp-Lys-NH₂
24

25
26
27 BE123: Ac-Nle-Asn-His-D-Phe-Arg-Trp-Lys(*N*^εAc)-NH₂
28
29

30
31
32 Table 1 reports the EC₅₀ values in the adenylyl cyclase based bioassays of the linear peptides:
33
34 the linear peptide precursors I'-X', the classical NDP-MSH, and the MT-II analogs – BE123 and
35
36 BE124. Peptide BE123 in which the charges on Asp and Lys present in BE124 are eliminated
37
38 reproduces closely the effect of side chain-to-side chain cyclization present in MT-II. As such,
39
40 short of the conformational rigidification, BE123 is a linear version of MT-II. Table 2
41
42 summarizes the functional agonist potencies of the 1,4- and 4,1-disubstituted-[1,2,3]triazolyl-
43
44 containing cyclopeptides I-X, compared to MT-II. In this study we used HEK-293 cells stably
45
46 expressing the murine melanocortin receptors subtypes mMC1R, mMC3R, mMC4R, and
47
48 mMC5R to assess the agonist potency and subtype selectivity profiles of these MT-II mimetic
49
50 peptides.^{28,29}
51
52
53
54
55
56
57
58
59
60

1
2
3 Among the linear peptides NDP-MSH is the most potent mMC1R agonist showing an EC_{50}
4 value that is 5- and 9-fold lower than the respective values for BE124 and BE123 (Table 1). All
5 three linear peptides are good agonists toward the mMCR4R with very similar subnanomolar
6 EC_{50} s (0.20-0.31 nM) and are 4-9-fold lower than their EC_{50} s toward mMC3R and mMC5R.
7
8 Relative to the linear peptides, the cyclic MT-II is the most potent agonist toward all four
9 receptor subtypes. It is about 2- and 4-fold more potent than NDP-MSH on the mMC1R and
10 mMC4R, respectively. Moreover, MT-II discriminates nicely between mMC1R or mMC4R and
11 mMC3R or mMC5R. Interestingly, both BE124 and its potential charge-bearing side chains
12 blocked variant BE123 are almost equipotent in all four receptor subtypes. Apparently, the
13 application of the conformational constraint in the form of i-to-i+5 side chain-to-side chain
14 lactam bridge formation as in MT-II and not the neutralization of potential charge-bearing
15 groups as in BE123 play a critical role in potentiation and enhancement of functional selectivity
16 toward certain receptor subtypes.
17
18
19
20
21
22
23
24
25
26
27
28
29
30
31
32
33

34 The potencies of the linear peptide precursors I'-X' (Table 1, Figure 1) span a range of two
35 orders of magnitude between the most potent one X' ($EC_{50} \approx 0.050$ nM in mMC4R and mMC5R)
36 and the least potent one II' ($EC_{50} = 5.33$ nM in mMC5R). Analog X' is the most potent on all four
37 receptor subtypes with 5-8-fold higher potency on mMC4R and mMC5R than on mMC1R and
38 mMC3R. The selectivity for receptor subtype of a single analog is in the range of 5-10-fold. For
39 example, IX' is 10-fold more potent in mMC5R than in mMC3R (EC_{50} s 0.23 and 2.33 nM,
40 respectively).
41
42
43
44
45
46
47
48
49
50
51
52
53
54
55
56
57
58
59
60

Table 1. Functional potency (EC_{50}) of linear peptide precursors N^{α} -Ac[Nle⁴,Yaa⁵,D-Phe⁷,Xaa¹⁰] α MSH(4-10)NH₂ (I', II', III', IV', and IX') and N^{α} -Ac[Nle⁴,Xaa⁵,D-Phe⁷,Yaa¹⁰] α MSH(4-10)NH₂ (V', VI', VII', VIII', and X'). EC_{50} of NDP-MSH, BE123, and BE124 are reported as references.

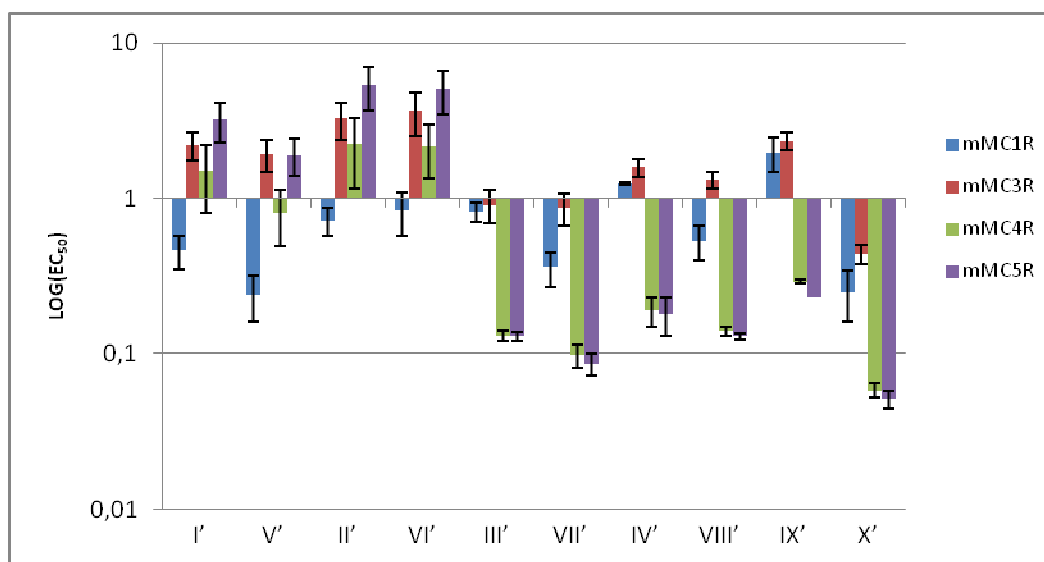
		mMC1R ^b	mMC3R ^b	mMC4R ^b	mMC5R ^b
code	[Xaa ⁵ ,Yaa ¹⁰] and [Yaa ⁵ ,Xaa ¹⁰] ^a	EC_{50} (nM)	EC_{50} (nM)	EC_{50} (nM)	EC_{50} (nM)
		\pm SEM	\pm SEM	\pm SEM	\pm SEM
I'	[Pra ⁵ ,Nle ¹⁰ (ϵ -N ₃)]	0.46 \pm 0.11	2.19 \pm 0.45	1.50 \pm 0.69	3.22 \pm 0.92
V'	[Nle ⁵ (ϵ -N ₃),Pra ¹⁰]	0.24 \pm 0.08	1.92 \pm 0.45	0.81 \pm 0.32	1.90 \pm 0.51
II'	[Hex ⁵ (5-ynoic),Nva ¹⁰ (δ -N ₃)]	0.72 \pm 0.15	3.27 \pm 0.88	2.22 \pm 1.06	5.33 \pm 1.65
VI'	[Nva ⁵ (δ -N ₃),Hex ¹⁰ (5-ynoic)]	0.83 \pm 0.26	3.66 \pm 1.16	2.15 \pm 0.81	5.04 \pm 1.59
III'	[Hept ⁵ (6-ynoic),hAla ¹⁰ (γ -N ₃)]	0.82 \pm 0.12	0.91 \pm 0.22	0.13 \pm 0.01	0.13 \pm 0.009
VII'	[hAla ⁵ (γ -N ₃),Hep ¹⁰ (6-ynoic)]	0.36 \pm 0.09	0.86 \pm 0.2	0.098 \pm 0.017	0.086 \pm 0.013
IV'	[Oct ⁵ (7-ynoic),Ala ¹⁰ (β -N ₃)]	1.24 \pm 0.027	1.58 \pm 0.2	0.19 \pm 0.04	0.18 \pm 0.049
VIII'	[Ala ⁵ (β -N ₃),Oct ¹⁰ (7-ynoic)]	0.53 \pm 0.13	1.32 \pm 0.16	0.14 \pm 0.009	0.13 \pm 0.006
IX'	[Hex ⁵ (5-ynoic),hAla ¹⁰ (γ -N ₃)]	1.98 \pm 0.50	2.33 \pm 0.31	0.29 \pm 0.009	0.23 \pm 0.002
X'	[hAla ⁵ (γ -N ₃),Hex ¹⁰ (5-ynoic)]	0.25 \pm 0.09	0.44 \pm 0.06	0.058 \pm 0.006	0.051 \pm 0.007

NDP-MSH ^c	0.092±0.027	0.81±0.30	0.20 ± 0.01	n.d. ^d
BE123 ^c	0.75 ± 0.17	2.4 ± 0.41	0.31 ± 0.02	n.d. ^d
BE124 ^c	0.46 ± 0.11	1.1 ± 0.10	0.21 ± 0.02	n.d. ^d

^a Notations: Pra – L-propargylglycine; Nva – L-norvaline; hAla – L-homoalanine; Hex – L- α -amino hexanoic acid; Hept – L- α -amino heptanoic acid; Oct – L- α -amino octanoic acid. ^b Agonist potencies (EC_{50}) of the lactam containing peptide (MT-II) in mMC1R, mMC3R, mMC4R, and mMC5R are 0.03, 0.18, 0.06, and 0.19 nM, respectively, ^c The detailed sequences are given in Scheme 4. ^d n.d. means not determined.

The melanocortin receptor subtype related potencies of the two short linear MT-II-related peptides BE123 and BE124 is very similar to that of the linear precursors I'-X' regardless of the nature of side-chain modifications in positions 5 and 10 (α -MSH-based numbering). Moreover, in general, most of the linear short α -MSH(4-10)-derived peptides are less potent than either MT-II or its cyclic heterodetic “clicked” MT-II-derived peptides I-X.

Figure 1: Logarithmic graphical representation of functional agonist activity (EC_{50} in nM) of linear peptide precursors (I' ÷ X').



Neither MT-II nor the 1,4- and 4,1-disubstituted-[1,2,3]triazolyl-containing cyclopeptides I-X show very high selectivity toward a specific receptor subtype and there is no consistent trend for receptor subtype selectivity in the [1,2,3]triazolyl-containing analog series (Table 2, Figure 2). For example, while MT-II is 3-6-fold more potent toward mMC1R and mMC4R (cf. EC_{50} s 0.03 and 0.06 nM on mMC1R and mMC4R, respectively, with 0.18 and 0.19 nM on mMC3R and mMC5R, respectively) the maximal selectivity observed for the least potent analogs I and V toward the different receptor subtypes is 2- to 3-fold and 3- to 6-fold, respectively, (EC_{50} s 1.62, 3.14, and 5.18 nM of analog I in mMC4R, mMC3R, and mMC1R, respectively, and 0.58, 1.76, and 3.70 nM of analog V in mMC4R, mMC5R, and mMC3R, respectively). The most potent [1,2,3]triazolyl-containing analogs in this series are III, IV, VII, and X. They all have preference to the mMC4R and mMC5R (EC_{50} s 0.051, 0.041, 0.048, and 0.067 nM, respectively, on the former receptor subtype, and 0.042, 0.035, 0.045, and 0.07 nM, respectively, on the latter one)

and analogs IV and VII are active to a lesser extent on mMC1R (EC_{50} s 0.087 and 0.074 nM, respectively).

Table 2. Agonist potency (EC_{50}) of the [1,2,3]triazolyl-containing cyclopeptides N^{α} -Ac[Nle⁴,Yaa⁵(&¹),D-Phe⁷,Xaa¹⁰(&²)] α MSH(4-10)NH₂ [$\{&^1(\text{CH}_2)_{n-1,4}$ -[1,2,3]triazolyl-(CH₂)_m&²\}] (I, II, III, IV, and IX) and N^{α} -Ac[Nle⁴,Xaa⁵(&¹),D-Phe⁷,Yaa¹⁰(&²)] α MSH(4-10)NH₂ [$\{&^1(\text{CH}_2)_{m-4,1}$ -[1,2,3]triazolyl-(CH₂)_n&²\}] (V, VI, VII, VIII, and X). EC_{50} of MT-II is reported as reference.

Code	[& ¹ (CH ₂) _{n-1,4} -[1,2,3]triazolyl-(CH ₂) _m & ²] and [& ¹ (CH ₂) _{m-4,1} -[1,2,3]triazolyl-(CH ₂) _n & ²]	mMC1R	mMC3R	mMC4R	mMC5R
		EC_{50} (nM) \pm SEM	EC_{50} (nM) \pm SEM	EC_{50} (nM) \pm SEM	EC_{50} (nM) \pm SEM
I	[& ¹ (CH ₂) _{1-1,4} -[1,2,3]triazolyl-(CH ₂) ₄ & ²]	5.18±0.54	3.14±0.25	1.62±0.57	1.93±0.07
V	[& ¹ (CH ₂) _{4-1,4} -[1,2,3]triazolyl-(CH ₂) ₁ & ²]	0.85±0.07	3.70±0.36	0.58±0.14	1.76±0.037
II	[& ¹ (CH ₂) _{2-1,4} -[1,2,3]triazolyl-(CH ₂) ₃ & ²]	0.11±0.029	0.29±0.1	0.22±0.06	0.34±0.09
VI	[& ¹ (CH ₂) _{3-4,1} -[1,2,3]triazolyl-(CH ₂) ₂ & ²]	0.71±0.11	1.91±0.73	0.85±0.36	1.88±0.70
III	[& ¹ (CH ₂) _{3-1,4} -[1,2,3]triazolyl-(CH ₂) ₂ & ²]	0.1±0.009	0.21±0.038	0.051±0.006	0.042±0.005
VII	[& ¹ (CH ₂) _{2-4,1} -[1,2,3]triazolyl-(CH ₂) ₃ & ²]	0.074±0.02	0.20±0.006	0.048±0.007	0.045±0.004
IV	[& ¹ (CH ₂) _{4-1,4} -[1,2,3]triazolyl-(CH ₂) ₁ & ²]	0.087±0.029	0.2±0.002	0.041±0.001	0.035±0.007
VIII	[& ¹ (CH ₂) _{1-4,1} -[1,2,3]triazolyl-(CH ₂) ₄ & ²]	0.53±0.14	0.60±0.04	0.14±0.02	0.13±0.015
IX	[& ¹ (CH ₂) _{2-1,4} -[1,2,3]triazolyl-(CH ₂) ₂ & ²]	0.32±0.097	0.63±0.13	0.14±0.029	0.15±0.02
X	[& ¹ (CH ₂) _{2-4,1} -[1,2,3]triazolyl-(CH ₂) ₂ & ²]	0.20±0.023	0.29±0.07	0.067±0.004	0.07±0.004

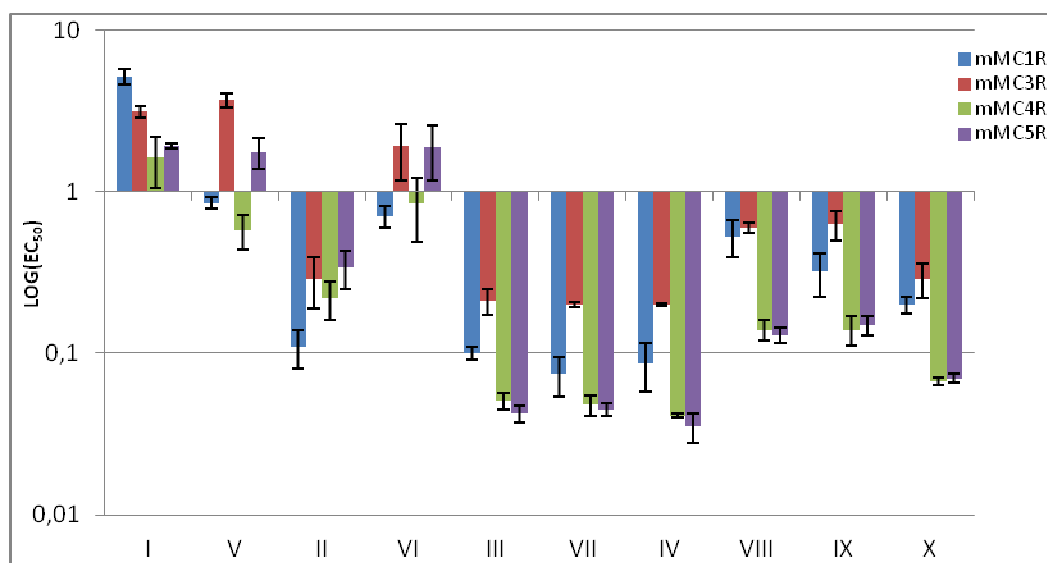
MT-II ^a	0.03±0.005	0.18±0.04	0.06±	0.19±0.05
--------------------	------------	-----------	-------	-----------

[1,2,3]Triazolyl-containing analogs I-VIII share a common location of the bridgeheads (positions 5 and 10) and an identical size of the bridges (5 methylenes in total and a 1,4-disubstituted [1,2,3]triazolyl moiety). As such, they are loosely reproducing the features of the lactam bridge in MT-II (5 methylenes in total and one amide bond). However, these heterodetic cyclopeptides differ in the location of the [1,2,3]triazolyl moiety within the bridge so it is removed one or two methylenes from the *N*-proximal bridgehead (analog I and VIII, and II and VII, respectively) or one or two methylenes from the *C*-proximal bridgehead (analog IV and V, and III and VI, respectively). The location of the [1,2,3]triazolyl moiety within the bridge in analogs I and VIII is identical with the location of the isosteric amide within the lactam bridge in MT-II. Evidently, I and VIII are less potent than MT-II in mMC1R, mMC3R, and mMC4R (Table 2). Moreover I, which incorporates a 4,1-[1,2,3]triazolyl moiety, is much less potent than VIII, which incorporates a 1,4-[1,2,3]triazolyl moiety. Interestingly, analog VII, which incorporates the 1,4-[1,2,3]triazolyl, is more potent than analog II, which incorporates the 4,1-[1,2,3]triazolyl moiety despite of the [1,2,3]triazolyl moiety at the same position in the bridge. In both pairs I and VIII, and II and VII, where the position of the [1,2,3]triazolyl ring is closer to the *N*-proximal bridgehead, the more potent analogs VII and VIII are those that incorporate the 1,4-[1,2,3]triazolyl moiety. On the contrary, in both pairs IV and V, and III and VI, where the position of the [1,2,3]triazolyl ring is closer to the *C*-proximal bridgehead, the more potent analogs III and IV are those that incorporate the 4,1-[triazolyl] moiety. Analog IX and X have a shorter bridge than analogs I-VIII (4 methylenes in total and a 1,4-disubstituted [1,2,3]triazolyl moiety) and the [1,2,3]triazolyl moiety is flanked by two methylenes on each side in either the

1
2
3
4
5
6
7
8
9
10
11
12
13
14
15
16
17
18
19
20
21
22
23
24
25
26
27
28
29
30
31
32
33
34
35
36
37
38
39
40
41
42
43
44
45
46
47
48
49
50
51
52
53
54
55
56
57
58
59
60

4,1- or 1,4-orientation. Moreover, analogs IX and X differ in the orientation of the [1,2,3]triazolyl moiety, which is positioned equal distance from the bridgeheads, being 4,1 in the former and 1,4 in the latter. While both IX and X are more potent at mMC4R and mMC5R than on mMC1R and mMC3R, the activities of analog IX and X differ by the latter being more potent at the two former receptor subtypes thus being more selective than analog IX. The potency profiles of analogs IX and X (EC_{50} s 0.32, 0.63, 0.14, 0.15 nM and 0.20, 0.29, 0.067, and 0.07 nM at mMC1R, mMC3R, mMC4R, and mMC5R, respectively), follows very closely that of the corresponding analogs VIII and III (EC_{50} s 0.53, 0.60, 0.14, and 0.13 nM and 0.1, 0.21, 0.051, and 0.042 nM at mMC1R, mMC3R, mMC4R, and mMC5R, respectively).

Figure 2: Logarithmic graphical representation of agonist potency (EC_{50} in nM) of the [1,2,3]triazolyl-containing cyclopeptides (I ÷ X).



50
51
52
53
54
55
56
57
58
59
60

Taken together, these results suggest that close proximity of the [1,2,3]triazolyl moiety to the *N*-proximal bridgehead especially in the 4,1-orientation is disruptive for activity at all four receptor subtypes (analogs I and VIII, respectively). Interestingly, close proximity of the [1,2,3]triazolyl moiety to the *C*-proximal bridgehead as in analogs V and IV, presenting the [1,2,3]triazolyl in

1
2
3 the respective 1,4- and 4,1-orientation, results in an opposite effect in which it is very disruptive
4 for the former and very accommodating for the latter for all four receptor subtypes. Of note is the
5 higher activity of the linear precursors I' and V' on the mMC1R as compared to the activity of
6 the corresponding [1,2,3]triazolyl-containing cyclopeptides I and V on the same receptor subtype
7 (EC₅₀s 0.46 and 0.24 nM vs 5.18 and 0.85 nM). This may be the result of the serious perturbation
8 imposed by the 4,1-[1,2,3]triazolyl moiety when it is adjacent to the *N*-proximal bridgehead and
9 to a lesser extent, regardless the orientation of the [1,2,3]triazolyl ring, when it is adjacent to the
10 *C*-proximal bridgehead.
11
12
13
14
15
16
17
18
19
20
21

22 The comparison of the activity profile of the linear peptide precursors and their corresponding
23 [1,2,3]triazolyl-containing cyclopeptides indicates the latter, in general, to be slightly more
24 potent. Clearly, the linear precursors are already very potent indicating that the conformational
25 rigidification in the cyclopeptide is not critical for their high potency. Moreover, only in very
26 few cases the linear precursor peptides are more potent than their corresponding [1,2,3]triazolyl-
27 containing cyclopeptides (cf. I' and V' with I and V in mMC1R, respectively).
28
29
30
31
32
33
34
35
36

37 **Conformational analysis.** In order to gain insight on the relationship among the specific
38 features of the [1,2,3]triazolyl-containing bridge, the potency and receptor subtype selectivity,
39 and the conformation, we selected to study in detail the conformations of three representative
40 heterodetic [1,2,3]triazolyl-containing cyclopeptides I, IV, and V. The selection includes the
41 least potent analog I, one of the most potent analogs IV, and analog V of intermediate potency.
42 In addition, while analogs I and IV incorporate the 4,1-[1,2,3]triazolyl moiety in proximity to the
43 *N*-proximal- and *C*-proximal-bridgehead, respectively, both analogs IV and V incorporate the
44 [1,2,3]triazolyl moiety at the *C*-proximal-bridgehead but at opposite orientations, 4,1- and 1,4-
45 respectively. We anticipated that the opposing location of the [1,2,3]triazolyl ring in the bridge
46
47
48
49
50
51
52
53
54
55
56
57
58
59
60

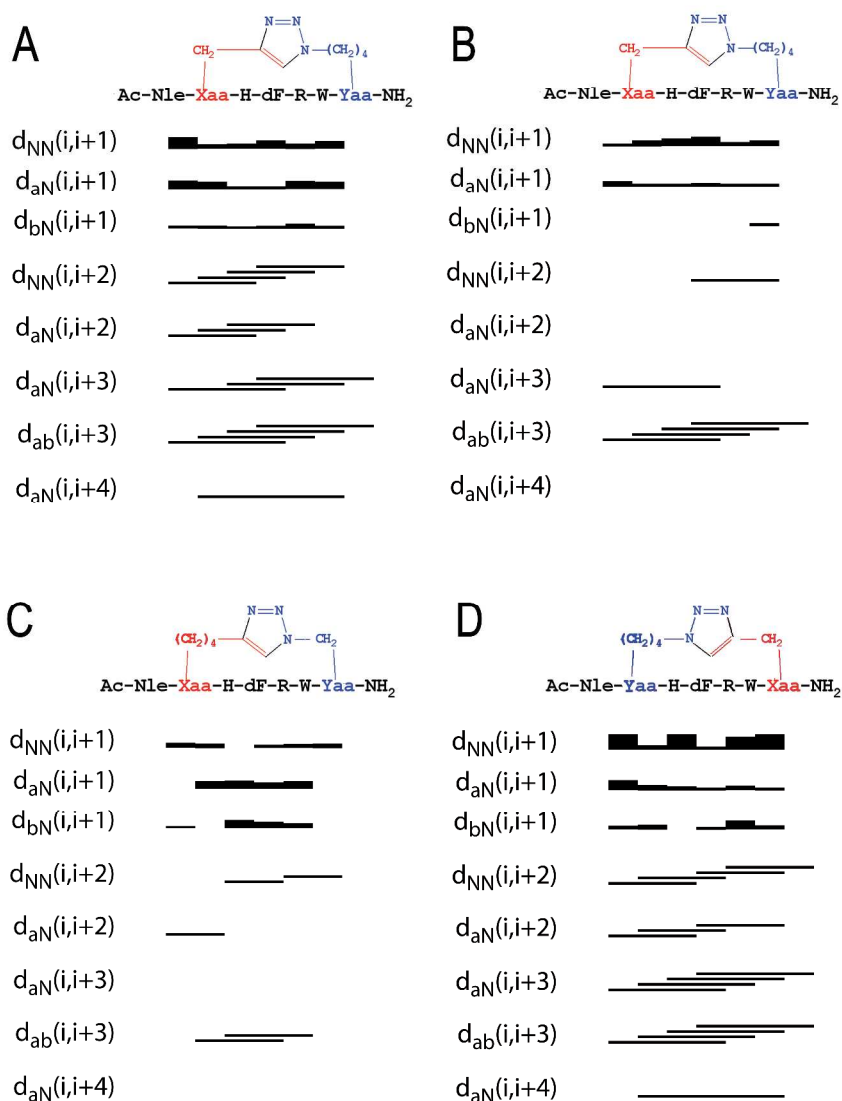
1
2
3 will affect the conformation to the extent that will explain the large difference in activity
4
5 between analogs I and IV. On the other hand, we speculate that the small difference in biological
6
7 activity between analogs IV and V, which share the same C-proximal bridgehead location of the
8
9 [1,2,3]triazolyl ring, may result in similar conformations in spite of the opposite orientations of
10
11 the [1,2,3]triazolyl ring within the bridge.
12
13

14
15 To allow comparison with the reported “bioactive” NMR solution structure(s) of the reference
16
17 homodetic cyclopeptide MT-II, the NMR spectra of the heterodetic cyclopeptides I, IV, and V
18
19 were acquired in DMSO-d₆.³⁰ Moreover, this polar, basic, and aprotic solvent was shown to
20
21 support intramolecular hydrogen bonds and prevent intermolecular aggregations.^{31,32} To exclude
22
23 potential aggregation, we recorded the 1D-¹H-NMR spectra of the clicked-cyclopeptides at a
24
25 concentration range spanning 1–0.1 mM. Importantly, at concentration of 0.1 mM there was no
26
27 indication for aggregation. Nevertheless, at 0.1 mM cyclopeptide I presented double signal
28
29 pattern spectra indicating the presence of two distinct populations of slow exchanging
30
31 conformations. Chemical shift assignments of the proton spectra were achieved via the standard
32
33 systematic application of DQF-COSY,³³ TOCSY,³⁴ and NOESY³⁵ experiments, using the
34
35 SPARKY³⁶ software package according to Wüthrich’s procedure.³⁷
36
37
38
39
40

41
42 Figure 3 reports sequential and medium range NOEs collected in NOESY spectra of
43
44 cyclopeptides I, IV, and V in DMSO-d₆ confirming the preliminary analysis of 1D-¹H-NMR
45
46 spectrum. Two NOEs bar diagrams are reported for [1,2,3]triazolyl-containing cyclopeptide I,
47
48 corresponding to the observed double signal pattern in the respective NOESY spectrum (Figure
49
50 3, panels A and B). The conformer IA is characterized by a more complete sequential and
51
52 medium range NOE pattern, while conformer IB shows less abundant and whenever observable
53
54 weak, sequential, and medium range connectivities. This observation is consistent with the
55
56
57
58
59
60

1
2
3 presence of the two predominant low energy conformational ensembles IA and IB, undergoing
4 slow dynamic interchange. We suggest that the markedly low potency of cyclopeptide I
5 compared to cyclopeptides IV and V in all melanocortin receptor subtypes (EC_{50} s 5.18, 3.14,
6 1.62, and 1.93 nM for mMC1R, mMC3, mMC4R, and mMC5R, respectively) can be attributed
7 to this conformational heterogeneity. NOE bar diagrams relative to cyclopeptides IV and V
8 (Figure 3, panels C and D, respectively), confirm the presence of numerous and diagnostic
9 sequential and medium range $i, i+2$ and $i, i+3$ NOE data in the corresponding NOESY spectra,
10 although a more regular and complete NOE patterns is observed for cyclopeptide V than for
11 cyclopeptide IV. NMR-derived models of cyclopeptides IA, IV, and V were calculated using
12 simulated annealing procedures imposing NOE-based inter-protonic distances as constraints.
13 Figure 4a shows the NMR-derived bundles of 20 low energy conformations of cyclopeptides IA,
14 IV, and V overlapping with the best calculated structure of MT-II. The NMR structure bundles
15 of cyclopeptides IA and V show high structural agreement with $RMSD \sim 0.50 \text{ \AA}$. In agreement
16 with the NOE bar diagrams reported in Figure 3, the structure bundle of cyclopeptide IV is
17 characterized by slightly higher RMSD value (0.80 \AA), indicating that cyclopeptide IV is more
18 flexible than cyclopeptides IA and V.
19
20
21
22
23
24
25
26
27
28
29
30
31
32
33
34
35
36
37
38
39
40
41
42
43
44
45
46
47
48
49
50
51
52
53
54
55
56
57
58
59
60

Figure 3. Sequential and medium-range NOEs for [1,2,3]triazolyl-containing cyclopeptides IA (Panel A), IB (Panel B), IV (Panel C), and V (Panel D). Panels A and B are derived from the NOE connectivities of the most (IA) and the lesser (IB) abundant conformers of I. Data were obtained from a 600 MHz NOESY experiments with a mixing time of 200 ms and collected in DMSO-d₆ at 300 K.

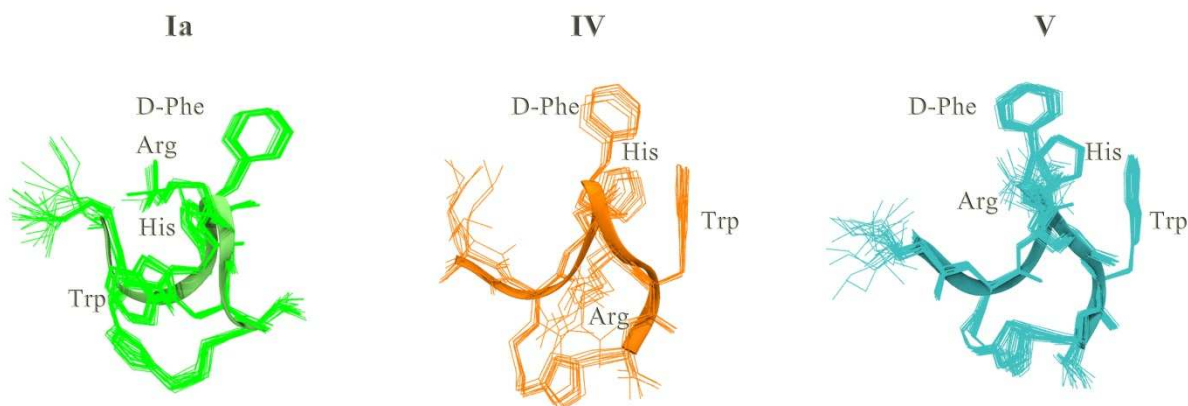


Quantitative analysis of ϕ and ψ (Supporting Information, Table 1s) dihedral angles of low-energy structures of cyclopeptides IA, IV, and V, using the PROMOTIF program (PROMOTIF-a

1
2
3 program to identify and analyze structural motifs in proteins)³⁸ highlights the preponderance of a
4 type I β -turn conformation centered on residues His⁶-Trp⁹. In agreement with the preliminary
5 analysis shown in the NOESY connectivity bar diagram (Figure 3), cyclopeptide IB appears to
6 be disordered presenting many irregular secondary structures including some transient α -helical
7 segments.
8
9
10
11
12
13

14
15 The comparison of the 20 lowest-energy NMR structures of cyclopeptides IA, IV, and V
16 (Figure 4a) suggests good overlap of the backbone atoms and a common orientation of His and
17 D-Phe side chains. Cyclopeptides IV and V show also a common orientation of the indol ring of
18 Trp.
19
20
21
22
23
24

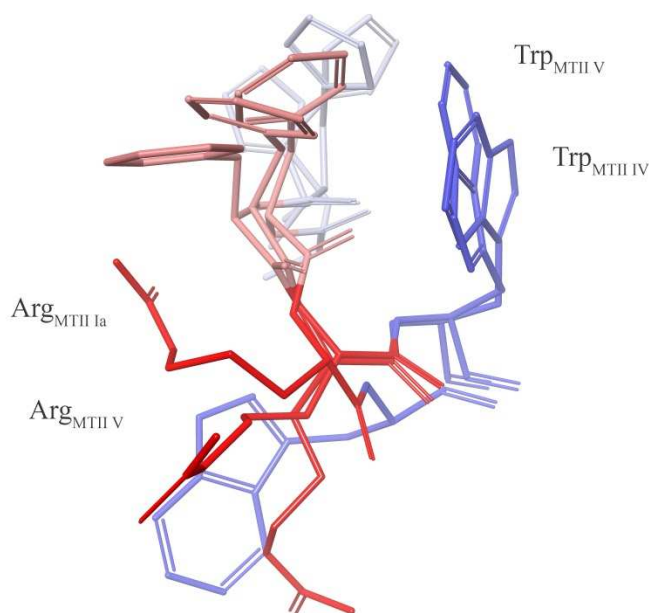
25
26 **Figure 4a:** Overlay of NMR-derived calculated structure bundles of IA, the most abundant
27 conformational ensemble (Panel A), IV (Panel B), and V (Panel C), all wireframe structures,
28 compared with the best calculated structure of MT-II (ribbon structure).
29
30
31
32
33



54 As shown in Figure 4b the Trp side chain of cyclopeptide IA points to an opposite direction as
55 compared to cyclopeptide IV and V. Moreover, the three cyclopeptides differ in the orientation
56
57
58
59
60

1
2
3 of the Arg side chain. In cyclopeptides IV and V, as documented by the relative NOE effects,
4 Arg side chains point to [1,2,3]triazolyl ring and D-Phe moiety, respectively (Figure 4a).
5
6 Consistent with the absence of NOEs suggesting proximity to other side chains, Arg side chain in
7
8 cyclopeptide IA, displays significantly higher flexibility than in analogs IV and V (Figures 4a
9
10 and 4b).

11
12
13
14
15
16 **Figure 4b:** Side chain orientation of cyclopeptides IA, IV, and V. Residue side chains are
17 colored as follow: L-His/light grey, D-Phe/pink, L-Arg/red, and L-Trp/blue



45
46 Stabilization of a type II β -turn because of D-Phe and the close proximity of His, D-Phe, and Trp
47 side chains on one of the homodetic cyclopeptide surface and Arg side chain on the opposite
48 surface in MT-II can explain the high potency and affinity to the melanocortin receptors.^{39,40} It is
49 known that a correct spatial orientation of the hydrophobic aromatic residues and the basic,
50 “arginine-like” moiety, are important for an effective interaction of MT-II and MT-II analogs at
51 the different MCR receptors.³⁰
52
53
54
55
56
57
58
59
60

1
2
3 In summary, conformational analysis of the three selected heterodetic [1,2,3]triazolyl-
4 containing MT-II analogs suggests that: i) the conformational polymorphism of cyclopeptide I
5 contributes to its overall low potency in all receptor subtypes as compared to the more
6 conformationally defined cyclopeptides IV and V; ii) the presence, location, and orientation of
7 the [1,2,3]triazolyl ring in the bridge does affect the spatial location of the side chains in general
8 and of the Arg side chain in particular. It appears that biological activity is derived from indirect
9 contribution to the spatial orientations of side chains more than by the direct interaction of the
10 bridge with the target receptor.
11
12
13
14
15
16
17
18
19
20
21

22 CONCLUSIONS

23
24 In the present paper we report for the first time a systematic structure-activity-conformation
25 relationship study in which a i-to-i+5 side chain-to-side chain Cu^I-catalyzed azido-to-alkyne 1,3-
26 dipolar cycloaddition (CuAAC) was performed in an attempt to reproduce a type I β-turn, which
27 is considered to be a critical feature in the putative bioactive conformation of MT-II. We
28 demonstrate that: 1) i-to-i+5 side chain-to-side chain CuAAC yields potent and interesting
29 melanocortin receptor agonists; 2) side chain-to-side chain conformational stabilization of type I
30 β-turn by i-to-i+5 side chain-to-side chain [1,2,3]triazolyl-containing bridges impacts the *in vitro*
31 potency and selectivity of these new stapled peptides at the different MCR receptor subtypes.
32 Relative to MT-II we frequently observe enhancement of potency at the mMC5R and loss of
33 potency at mMC1R; 3) Similar to the general enhancement of potency as a result of homodetic
34 side chain-to-side chain cyclization (cf. BE124 and BE123 with MT-II, Table I) we also observe
35 enhancement of potency upon transforming the linear precursors I'-X' to the heterodetic
36 [1,2,3]triazolyl-containing cyclopeptides. Interestingly, similar observation was reported by Cho
37 et al. in i-to-i+5 disulfide-bridged cyclic MSH peptides;⁴¹ 4) Regardless of the nature of i-to-i+5
38
39
40
41
42
43
44
45
46
47
48
49
50
51
52
53
54
55
56
57
58
59
60

1
2
3 side chain-to-side chain cyclizations their contribution to the stability of the critical type I β -turn
4
5 contributes to the enhancement of their agonist potency at all MCRs. Our observations concur
6
7
8 with those that propose side chain orientation of residues within the cyclic segment and those
9
10 that are flanking it to play a predominant role in determining receptor subtype selectivity. As
11
12 such, the *i*-to-*i*+5 side chain-to-side chain CuAAC offers obvious advantages over the more
13
14 traditional side chain-to-side chain cyclizations. These heterodetic [1,2,3]triazolyl-containing
15
16 MT-II mimetics can be constructed by taking advantage of the chemical orthogonality of the
17
18 azido and alkynyl functions, which reduces synthetic complexity. Moreover our approach offers
19
20 access to a vast structural diversity presented by the size of the bridge, the location and the
21
22 orientation of the [1,2,3]triazolyl moiety within the ring. In the future, we will seek to reduce the
23
24 size of the [1,2,3]triazolyl-containing bridge to achieve greater structural rigidification and
25
26 diversify the nature of the residues flanking the cyclic segment in order to achieve greater
27
28 receptor subtype selectivity.
29
30
31
32
33

34 35 **EXPERIMENTAL SECTION**

36
37 **Materials and methods.** The ω -alkynyl-alcohols, were purchased from Alfa Aesar; Fmoc-L-
38
39 Trp-(Boc)-OH, Fmoc-D-Phe-OH and Fmoc-L-Pra-OH amino acids, Fmoc-Rink amide resin and
40
41 HOBt were purchased from Iris Biotech GmbH (Marktredwitz, Germany); Fmoc-L-Arg(Pbf)-OH
42
43 and Fmoc-L-His(Trt)-OH amino acids were purchased from CBL (Patras, Greece); Fmoc-L-Nle
44
45 was purchased from NeOMPS (Strasbourg, France); TBTU from Advanced Biotech Italy (Milan,
46
47 Italy). Peptide-synthesis grade *N,N*-dimethylformamide (DMF) was purchased from Scharlau
48
49 (Barcelona, Spain); Acetonitrile from Carlo Erba (Milan, Italy); dichloromethane (DCM),
50
51 trifluoroacetic acid (TFA), piperidine, acetic anhydride (Ac₂O) and *N*-methyl morpholine
52
53 (NMM) were purchased from Sigma Aldrich (Milan, Italy). The scavengers for cleavage of
54
55
56
57
58
59
60

1
2
3 peptides from resin: 1,2-ethanedithiol (EDT), thioanisole, and phenol (PhOH), were purchased
4
5 from Acros Organics (Geel, Belgium), Jansenn Chimica (Beerse, Belgium), and Carlo Erba
6
7 (Milan, Italy).
8
9

10 The purity of the final linear precursors (I'-X') and the [1,2,3]triazolyl-containing MT-II
11
12 analogs (I-X) was established by analytical RP-HPLC and exceeded 95%, their structural
13
14 integrity was established by ESI-MS.
15
16
17

18 **Synthesis of N^{α} -Fmoc-Xaa(ω -N₃)-OH and N^{α} -Fmoc-Yaa(ω -yl)-OH.** N^{α} -Fmoc- ω -azido- α -
19
20 amino- and N^{α} -Fmoc- ω -ynoic- α -amino acids (1-4 and 5-7, respectively), with (CH₂)_{n/m} n/m = 1-4
21
22 in the side chain, were synthesized as described before.^{21,22} In particular, N^{α} -Fmoc- ω -azido- α -
23
24 amino acids were obtained by diazo-transfer from correspondent N^{α} -Fmoc- ω -amino- α -amino
25
26 acids; N^{α} -Fmoc- ω -ynoic- α -amino acids were obtained by alkylation of a Ni(II) complex of the
27
28 Schiff base derived from glycine and the chiral inducer (S)-2-(N-
29
30 benzylpropyl)aminobenzophenone with alk- ω -ynyl bromides.
31
32
33
34
35

36 **Synthesis of N^{α} -Ac[Nle⁴,Yaa⁵,D-Phe⁷,Xaa¹⁰] α MSH(4-10)NH₂ (I', II', III', IV', IX'), and**
37
38 **N^{α} -Ac-[Nle⁴,Xaa⁵,D-Phe⁷,Yaa¹⁰] α MSH(4-10)NH₂ (VI', V', VII', VIII', X').** Peptides I'-X'
39
40 were synthesized on a manual batch synthesizer (PLS 4X4, Advanced ChemTech) employing
41
42 Fmoc/tBu chemistry. The syntheses were performed on Rink-amide NovaSyn TGR resin (0.14
43
44 mmol/g, 300 mg). The Fmoc-Rink-amide resin was swelled with DMF (1 mL/100 mg of resin)
45
46 for 20 min before use. Stepwise peptide assembly was performed by repeating for each added
47
48 amino acid the following deprotection-coupling cycle: 1) Swelling: DMF (1 mL/100 mg of resin)
49
50 for 5 min; 2) Fmoc-deprotection: resin was washed twice with 20% (v/v) piperidine in DMF (1
51
52 mL/100 mg of resin, one wash for 5 min followed by another wash for 20 min); 3) Resin
53
54 washing: DMF (3-5 min); 4) Coupling: scale employed TBTU/HOBt/NMM (2.5:2.5:3.5 equiv.)
55
56
57
58
59
60

1
2
3 as the coupling system and 2.5 equiv. of the Fmoc protected amino acids, except for the
4 unnatural amino acids N^{α} -Fmoc-Xaa(ω -N₃)-OH and N^{α} -Fmoc-Yaa(ω -yl)-OH, for which 1.5
5 equiv. were used. The coupling was carried out in DMF (1 mL/100 mg of resin) for 50 min; 5)
6 Resin washings: DMF (3-5 min) and DCM (1-5 min). Each coupling was monitored by Kaiser
7 test⁴² and was negative, therefore recouplings were not needed. Acetylation of the amino
8 terminus was carried out in the presence of Ac₂O/NMM in DCM (20 equiv. 1.6 mL of DCM).
9 The reaction was monitored by Kaiser test.
10
11
12
13
14
15
16
17
18
19

20
21 **Deprotection, Cleavage, and Purification of Peptides. General Procedure.** Peptide
22 cleavage from the resin and simultaneous deprotection of the amino acid side chains were carried
23 out with a mixture of TFA/anisole/1,2-ethanedithiol/phenol/H₂O (94:1:1:1:1 v/v/v/v/v, 1 mL/100
24 mg of resin-bound peptide). The cleavage was carried out for 3 h with vigorous shaking at room
25 temperature. Resin was filtered and washed with TFA. The filtrate was concentrated under N₂
26 stream, addition of cold diethyl ether resulted in a precipitate that was separated by
27 centrifugation, dissolved in H₂O and lyophilized on an Edwards apparatus, model Modulyo.
28 Lyophilized crude peptides were pre-purified by solid-phase extraction with a RP-18 LiChroprep
29 silica column from Merck (Darmstadt, Germany) using H₂O/ACN as eluents. The final
30 purification of the peptides was performed by semi-preparative RP-HPLC on a Phenomenex
31 Jupiter C-18 (250 × 4.6 mm) column at 28 °C using a Waters instrument (Separation Module
32 2695, detector diode array 2996) working at 4 mL/min. The solvent systems used were: A (0.1%
33 TFA in H₂O) and B (0.1% TFA in CH₃CN). Final purity of all peptides was ≥95%. Peptides
34 were characterized by RP-HPLC ESI-MS. HPLC system is an Alliance Chromatography
35 (Waters) with a Phenomenex Kinetex C-18 column 2.6 μ m (100 × 3.0 mm) working at 0.6
36
37
38
39
40
41
42
43
44
45
46
47
48
49
50
51
52
53
54
55
56
57
58
59
60

1
2
3 mL/min, with UV detection at 215 nm, coupled to a single quadrupole ESI-MS (Micromass ZQ).
4
5 The solvent systems used were: A (0.1% TFA in H₂O) and B (0.1% TFA in CH₃CN).
6
7
8
9

10 **Synthesis of *N*^α-Ac[Nle⁴,Yaa⁵(&¹),D-Phe⁷,Xaa¹⁰(&²)]αMSH(4-10)NH₂ [{{&¹(CH₂)_n-1,4-**
11 **[1,2,3]triazolyl-(CH₂)_m&²}] (I, II, III, IV, IX) and *N*^α-Ac[Nle⁴,Xaa⁵(&¹),D-**
12 **Phe⁷,Yaa¹⁰(&²)]αMSH(4-10)NH₂ [{{&¹(CH₂)_m-1,4-[1,2,3]triazolyl-(CH₂)_n&²}] (V, VI, VII,**
13 **VIII, X).** Purified linear peptide precursors I'-X' (>95% purity) were subjected to intramolecular
14
15 Cu^I-catalyzed side-chain-to-side-chain azide-alkyne 1,3-dipolar Huisgen cycloaddition
16
17 (CuAAC). To a solution of the purified linear peptide (4.77 μmol) in H₂O/tBuOH (5 mL, 2:1
18
19 v/v) were added CuSO₄•5H₂O (40 μmol) and ascorbic acid (40.3 μmol). The mixture was stirred
20
21 overnight at room temperature, concentrated, and lyophilized. Complete and clean conversion of
22
23 all linear precursors into the desired [1,2,3]triazolyl-containing cyclopeptides I-X (Schemes 1
24
25 and 2) was observed. The cyclization was monitored by RP-HPLC ESI-MS. The crude
26
27 [1,2,3]triazolyl-containing cyclopeptides were purified (>97% purity) by solid-phase extraction
28
29 (SPE) on RP (C18) column, with CH₃CN in H₂O as eluents. The copper salts were removed by
30
31 elution with H₂O, whereas the desired cyclopeptides were eluted with CH₃CN/H₂O mixture.
32
33 Peptides were purified and characterized by semi-preparative RP-HPLC and RP-HPLC ESI-MS,
34
35 respectively.
36
37
38
39
40
41
42
43
44
45

46 **Solid Phase Synthesis of MT-II: *N*^α-Ac[Nle⁴-c(Asp⁵-D-Phe⁷-Lys¹⁰)]αMSH(4-10)NH₂.** The
47
48 fully protected resin-bound peptide was synthesized using a Rink-amide NovaSyn TGR resin
49
50 (0.63 mmol/g, 300 mg) on a manual batch synthesizer (PLS 4X4, Advanced ChemTech)
51
52 applying the Fmoc/tBu SPPS procedure, as previously reported. The coupling of *N*^α-Fmoc-amino
53
54 acids was performed using TBTU/HOBt/NMM (2.5 equiv.: 2.5 equiv.: 3.5 equiv.) and 2.5 equiv.
55
56
57
58
59
60

1
2
3 of each Fmoc protected amino acids. The coupling was carried out in DMF (1 mL/100 mg of
4 resin) for 40 min. The formation of the lactam bridges between side chains of Lys¹⁰ and Asp⁵
5 was performed on the resin-bound peptide, following an orthogonal protocol of deprotection. In
6 particular, Lys¹⁰ and Asp⁵ were protected on side chain respectively with 1-[(4,4-dimethyl-2,6-
7 dioxocyclohex-1-ylidene)ethyl] group (Dde) and with β -4-{N-[1-(4,4-dimethyl-2,6-
8 dioxocyclohexylidene)-3-methylbutyl]-amino} benzyl ester (ODmab), stable under the
9 conditions of peptide elongation. After acetylation of the *N*-terminal, Dde and ODmab were
10 removed by two consecutive steps, using hydrazine 20% in DMF (1 mL), first for 5 min,
11 followed by an additional step with freshly prepared deprotection mixture for 15 min. After
12 deprotection of Lys¹⁰ and Asp⁵, the formation of intramolecular lactam bridge was performed
13 using TBTU/HOBt/NMM (2.5:2.5:3.5 equiv.) as coupling system in DMF for 40 min. The
14 cyclization reaction was monitored by Kaiser test and by RP-HPLC ESI-MS analysis of MW-
15 assisted mini-cleavage resin-bound fragment. Mini-cleavage was carried out with TFA/TIS/water
16 solution (95:2.5:2.5 v/v/v), using a DiscoverTMS-Class single-mode MW reactor equipped with
17 Explorer-48 autosampler (CEM). The reaction was performed at 45 °C, using 15W for 15 min.
18 The reaction mixture was then filtered and the crude peptide was precipitated from the cleavage
19 mixture by addition of ice-cold diethyl ether followed by cooling for 5 min at -20 °C. The
20 product was collected by centrifugation and directly subjected to RP-HPLC ESI-MS analysis.
21
22
23
24
25
26
27
28
29
30
31
32
33
34
35
36
37
38
39
40
41
42
43
44
45

46
47 **Biological activity.** cAMP Based Functional Bioassay- HEK-293 cells stably expressing the
48 mouse melanocortin receptors were transiently transfected with 4 μ g CRE/ β -galactosidase
49 reporter gene as previously described.^{28,29,43,44} Briefly, 5,000 to 15,000 post transfection cells
50 were plated into collagen treated 96 well plates (Nunc) and incubated overnight.
51
52
53
54
55
56
57
58
59
60

Forty-eight hours post-transfection the cells were treated with 100 μL peptide (10^{-6} - 10^{-12} M) or forskolin (10^{-4} M) as a control in assay medium (DMEM containing 0.1 mg/mL BSA and 0.1 mM isobutylmethylxanthine) for 6 h. The assay media was aspirated and 50 μL of lysis buffer (250 mM Tris-HCl pH=8.0 and 0.1% Triton X-100) was added. The plates were stored at -80 $^{\circ}\text{C}$ overnight. The plates containing the cell lysates were thawed the following day. Aliquots of 10 μL were taken from each well and transferred to another 96-well plate for relative protein determination. To the cell lysate plates, 40 μL phosphate-buffered saline with 0.5% BSA was added to each well. Subsequently, 150 μL substrate buffer (60 mM sodium phosphate, 1 mM MgCl_2 , 10 mM KCl, 5 mM β -mercaptoethanol, 2 mg/mL ONPG) was added to each well and the plates were incubated at 37 $^{\circ}\text{C}$. The sample absorbance, OD_{405} , was measured using a 96 well plate reader (Molecular Devices). The relative protein concentration was determined by adding 200 μL 1:5 dilution Bio Rad G250 protein dye:water to the 10 μL cell lysate sample taken previously, and the OD_{595} was measured on a 96 well plate reader (Molecular Devices). Data points were normalized to the relative protein content. EC_{50} values represent the mean of three or more independent experiments. EC_{50} estimates, and their associated standard errors of the mean, were determined by fitting the data to a nonlinear least-squares analysis using the PRISM program (v4.0, GraphPad Inc.).

NMR conformational analysis. Samples for NMR were prepared by dissolving 1.2 mg of the lactam- and heterodetic [1,2,3]triazolyl-containing cyclo-heptapeptides in 0.5 mL of aqueous phosphate buffer (pH 6.6, 100 mM). Samples were lyophilized and dissolved in a mixture of DMSO/water (0.5 mL, 80:20, v/v). NMR spectra were recorded on a Bruker DRX-600 spectrometer. To exclude potential aggregation, One-dimensional (^1D) proton spectra of the cyclopeptides at a concentration range spanning 0.1–1 mM were recorded. At a peptide

1
2
3 concentration of 0.1 mM, the peptides did not display any noticeable effects of aggregation. ¹D
4
5 NMR spectra were recorded in the Fourier mode with quadrature detection. The water signal was
6
7 suppressed by a low-power selective irradiation in the homogated mode. DQF-COSY, TOCSY,
8
9 and NOESY experiments were run in the phase-sensitive mode using quadrature detection in ω_1
10
11 by time-proportional phase incrementation of the initial pulse. Data block sizes comprised of
12
13 2048 addresses in t2 and 512 equidistant t1 values. Before Fourier transformation, the time
14
15 domain data matrices were multiplied by shifted sin² functions in both dimensions. A mixing
16
17 time of 70 ms was used for the TOCSY experiments. NOESY experiments were run at 300 K
18
19 with mixing times in the range of 100-250 ms. The qualitative and quantitative analyses of DQF-
20
21 COSY, TOCSY and NOESY spectra were obtained using the SPARKY interactive program
22
23 package. Complete proton resonance assignments were achieved following Wüthrich's
24
25 procedure. Sequential and medium range Nuclear Overhauser Effects (NOEs)-derived distances
26
27 were used to generate 3D-models of the heterodetic [1,2,3]triazolyl-containing cyclo-
28
29 heptapeptides. The final pdb files were analyzed and validated using PROMOTIF software.
30
31
32
33
34
35
36

37 **NMR structure calculation.** On the basis of sequential and medium range NOE derived
38
39 distances, 3D models of lactam- and [1,2,3]triazolyl-containing peptides were generated with a
40
41 simulated annealing procedure using the DYANA software package. All structures were energy
42
43 minimized with the SANDER module of the AMBER 5 program, using for 1000 steps the
44
45 steepest descent method and for 4000 steps the conjugate gradient method. A non-bonded cut-off
46
47 of 12 Å and a distance-dependent dielectric term ($\epsilon = 4 * r$) were used. The minimization protocol
48
49 included three steps in which NOE derived distances were used as constraints with a force
50
51 constant, respectively, of 1000, 100, and 10 kcal/molÅ. The final pdb files were analyzed and
52
53 validated using PROCHECK software.
54
55
56
57
58
59
60

1
2
3
4
5
6 **ASSOCIATED CONTENT**
7

8
9 **Supporting Information.** Products characterization and NMR data. This material is available
10 free of charge via the Internet at <http://pubs.acs.org>.
11
12
13

14
15
16
17
18 **AUTHOR INFORMATION**
19

20
21 **Corresponding Authors**
22

23
24 *annamaria.papini@unifi.it
25

26
27
28 *michael_chorev@hms.harvard.edu
29
30
31
32

33
34 **Author Contributions**
35

36 The manuscript was written through contributions of all authors. All authors have given approval
37 to the final version of the manuscript.
38
39
40
41
42
43
44

45
46 **Funding Sources**
47

48 This work was partially supported by the "Programme de cotutelle internationale de thèse de
49 doctorat soutenu par la Région Ile-de-France, for the PhD of CT; by Agence Nationale de la
50 Recherche "Programme Chaire d'Excellence" ANR-09-CEXC-013-01 to AMP, and by the
51
52
53
54
55
56
57
58
59
60
Fondazione Ente Cassa di Risparmio di Firenze (Italy) to PeptLab@UniFi. The biological part
has been supported by NIH Grant R01DK091906 (CHL).

ACKNOWLEDGMENT

We thank Dr. Debora D'Addona and Dr. Susanna Mazzoni for their technical support in the preparing the α -alkynyl α -amino acids.

ABBREVIATIONS

ACN, acetonitrile; CuAAC, Cu^I-catalyzed azido-to-alkyne 1,3-dipolar cycloaddition; DCM, dichloromethane; DMF, *N,N*-dimethylformamide; EDT, 1,2-ethanedithiol; ESI-MS, electron-spray ionization mass spectrometry; GPCR, G protein-coupled receptors; HOBT, *N*-hydroxybenzotriazole; MCR, Melanocortin GPCR receptors; MSH, Melanocortin stimulating hormones; MT-II, melanotan II; NDP- α -MSH, Norleucine-4, D-Phe-7 α -MSH(1-13); NMM, *N*-methyl morpholine; POMC, pro-opiomelanocortin prohormone; Pra, *N*-propargyl glycine; PTHrP, parathyroid hormone-related protein; SAR, Structure-activity relationships; TBTU, 1-[bis(dimethylamino)methylene]-1H-benzotriazolium 3-oxide tetrafluoroborate; TFA, trifluoroacetic acid; UPLC, ultraperformance liquid chromatography.

REFERENCES

- (1) Chhajlani, V.; Wikberg, J. E. Molecular cloning and expression of the human melanocyte stimulating hormone receptor cDNA. *FEBS Lett.* **1992**, *309*, 417-420.
- (2) Gantz, I.; Miwa, H.; Konda, Y.; Shimoto, Y.; Tashiro, T.; Watson, S. J.; Del Valle, J.; Yamada, T. Molecular cloning, expression, and gene localization of a fourth melanocortin receptor. *J. Biol. Chem.* **1993**, *268*, 15174-15179.

- 1
2
3
4
5
6
7
8
9
10
11
12
13
14
15
16
17
18
19
20
21
22
23
24
25
26
27
28
29
30
31
32
33
34
35
36
37
38
39
40
41
42
43
44
45
46
47
48
49
50
51
52
53
54
55
56
57
58
59
60
- (3) Wessells, H.; Hruby, V. J.; Hackett, J.; Han, G.; Balse-Srinivasan, P.; Vanderah, T. W. Ac-Nle-c[Asp-His-DPhe-Arg-Trp-Lys]-NH₂ induces penile erection via brain and spinal melanocortin receptors. *Neuroscience* **2003**, *118*, 755-762.
- (4) Fan, W.; Boston, B. A.; Kesterson, R. A.; Hruby, V. J.; Cone, R. D. Role of melanocortineric neurons in feeding and the agouti obesity syndrome. *Nature* **1997**, *385*, 165-168.
- (5) Huszar, D.; Lynch, C. A.; Fairchild-Huntress, V.; Dunmore, J. H.; Fang, Q.; Berkemeir, L. R.; Gu, W.; Kesterson, R. A.; Boston, B. A.; Cone, R. D.; Smith, F. J.; Campfield, L. A.; Burn, P.; Lee, F. Targeted disruption of the melanocortin-4 receptor results in obesity in mice. *Cell* **1997**, *88*, 131-141.
- (6) Mogil, J. S.; Wilson, S. G.; Chesler, E. J.; Rankin, A. L.; Nemmani, V. S.; Lariviere, W. R.; Groce, M. K.; Wallace, M. R.; Kaplan, L.; Staud, R.; Ness, T. J.; Glover, T. L.; Stankova, M.; Mayorov, A. V.; Hruby, V. J.; Grisel, J. E.; Fillingim, R. B. The melanocortin-1 receptor gene mediates female-specific mechanisms of analgesia in mice and humans. *Proc. Natl. Acad. Sci. U.S.A.* **2003**, *100*, 4867-4872.
- (7) Chen, A. S.; Marsh, D. J.; Trumbauer, M. E.; Frazier, E. G.; Guan, X. M.; Yu, H.; Rosenblum, C. I.; Vongs, A.; Feng, Y.; Cao, L.; Metzger, J. M.; Strack, A. M.; Camacho, R. E.; Mellin, T. N.; Nunes, C. N.; Min, W.; Fisher, J.; Gopal-Truter, S.; Mac Intyre, D. E.; Chen, H. Y.; Van der Ploeg, L. H. Inactivation of the mouse melanocortin-3 receptor results in increased fat mass and reduced lean body mass. *Nat. Genet.* **2000**, *26*, 97-102.

- 1
2
3
4
5
6
7
8
9
10
11
12
13
14
15
16
17
18
19
20
21
22
23
24
25
26
27
28
29
30
31
32
33
34
35
36
37
38
39
40
41
42
43
44
45
46
47
48
49
50
51
52
53
54
55
56
57
58
59
60
- (8) Butler, A. A.; Kesterson, R. A.; Khong, K.; Cullen, M. J.; Pelleymounter, M. A.; Dekoning, J.; Baetscher, M.; Cone, R. D. A unique metabolic syndrome causes obesity in the melanocortin-3 receptor-deficient mouse. *Endocrinology* **2000**, *141*, 3518-3521.
- (9) Hruby, V. J.; Wilkes, B. C.; Cody, W. L.; Sawyer, T. K.; Hadley, M. E. Melanotropins: structural, conformational and biological considerations in the development of superpotent and superprolonged analogs. *Pept. Protein Rev.* **1984**, *3*, 1-64.
- (10) Mountjoy, K. G.; Robbins, L. S.; Mortrud, M. T.; Cone, R. D. The cloning of a family of genes that encode the melanocortin receptors. *Science* **1992**, *257*, 1248-1251.
- (11) Holder, J. R.; Haskell-Luevano, C. Melanocortin ligands: 30 years of structure-activity relationship (SAR) studies. *Med. Res. Rev.* **2004**, *24*, 325-356.
- (12) Lam, D. D.; Farooqi, I. S.; Hesler, L. K. Melanocortin receptors as targets in the treatment of obesity. *Curr. Top. Med. Chem.* **2007**, *7*, 1085-1097.
- (13) Haskell-Luevano, C.; Nichiforovich, G.; Sharma, S. D.; Yang, Y. K.; Dickinson, C.; Hruby, V. J.; Gantz, I. Biological and conformational examination of stereochemical modifications using the template melanotropin peptide, Ac-Nle-c[Asp-His-Phe-Arg-Trp-Ala-Lys]-NH₂, on human melanocortin receptors. *J. Med. Chem.* **1997**, *40*, 1738-1748.
- (14) Al-Obeidi, F. A.; Hadley, M. E.; Pettitt, M. B.; Hruby, V.J. Design of a new class of superpotent cyclic α -melanotropins based on quenched dynamic simulations. *J. Am. Chem. Soc.* **1989**, *111*, 3413-3416.

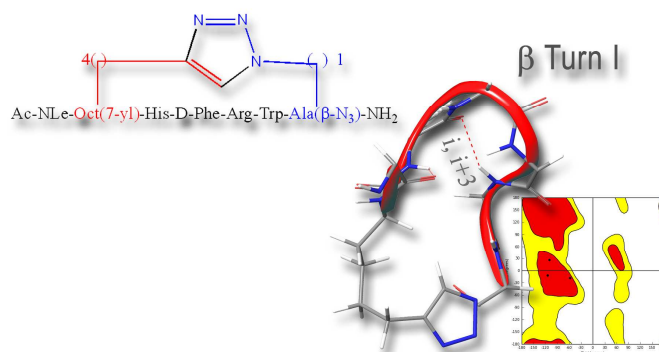
- 1
2
3 (15) Al-Obeidi, F. A.; Castrucci, A. L.; Hadley, M. E. Potent and prolonged acting cyclic lactam
4 analogues of alpha-melanotropin: design based on molecular dynamics. *J. Med. Chem.*
5 **1989**, *32*, 2555-2561.
6
7
8
9
10
11 (16) Ying, J.; Kövér, K. E.; Gu, X.; Han, G.; Trivedi, D. B.; Kavarana, M. J.; Hruby, V. J.
12 Solution structures of cyclic melanocortin agonists and antagonists by NMR. *Biopolymers*
13 **2003**, *71*, 696-716.
14
15
16
17
18
19 (17) Henchey, L. K.; Jochim, A. L.; Arora, P. S. Contemporary strategies for the stabilization of
20 peptides in the alpha-helical conformation. *Curr. Opin. Chem. Biol.* **2008**, *12*, 692-697.
21
22
23
24
25 (18) Kim, Y. W.; Verdine, G. L. Stereochemical effects of all-hydrocarbon tethers in $i,i+4$
26 stapled peptides. *Bioorg. Med. Chem. Lett.* **2009**, *19*, 2533-2536.
27
28
29
30 (19) Cantel, S.; Le Chavelier Isaad, A.; Scrima, M.; Levy, J. J.; Di Marchi, R. D.; Rovero, P.;
31 Halperin, J. A.; D' Ursi, A. M.; Papini, A. M.; Chorev, M. Synthesis and conformational
32 analysis of a cyclic peptide obtained via i to $i+4$ intramolecular side-chain to side-chain
33 azide-alkyne 1,3-dipolar cycloaddition. *J. Org. Chem.* **2008**, *73*, 5663-5674.
34
35
36
37
38
39
40 (20) Spengler, J., Jimenez, J.-C., Burger, K., Giralt, E., Albericio, F. Abbreviated nomenclature
41 for cyclic and branched homo- and hetero-detic peptides. *J. Peptide Res.* **2005**, *65*, 550-
42 555.
43
44
45
46
47
48 (21) Le Chevalier Isaad, A.; Papini, A. M.; Chorev, M.; Rovero, P. Side chain-to-side chain
49 cyclization by click reaction. *J. Pept. Sci.* **2009**, *15*, 451-454.
50
51
52
53
54
55
56
57
58
59
60

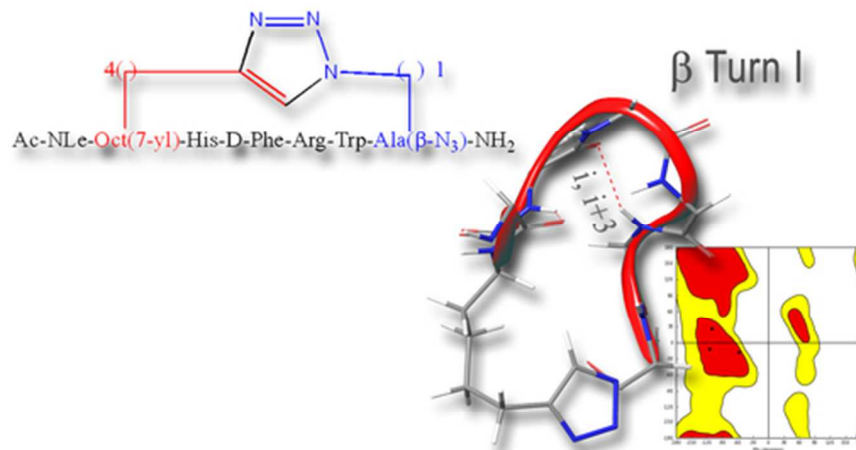
- 1
2
3
4
5
6
7
8
9
10
11
12
13
14
15
16
17
18
19
20
21
22
23
24
25
26
27
28
29
30
31
32
33
34
35
36
37
38
39
40
41
42
43
44
45
46
47
48
49
50
51
52
53
54
55
56
57
58
59
60
- (22) Le Chevalier Isaad, A.; Barbetti, F.; Rovero, P.; D'Ursi, A. M.; Chelli, M.; Chorev, M.; Papini, A. M. N^α -Fmoc-Protected ω -azido- and ω -alkynyl-L-amino acids as building blocks for the synthesis of "clickable" peptides. *Eur. J. Org. Chem.* 2008, *31*, 5308-5314.
- (23) Merrifield, R. B. Solid phase peptide synthesis. I. The synthesis of a tetrapeptide. *J. Am. Chem. Soc.* **1963**, *85*, 2149-2154.
- (24) Kolb, H. C.; Finn, M. G.; Sharpless, K. B. Click Chemistry: Diverse chemical function from a few good reactions. *Angew. Chem., Int. Ed. Engl.* **2001**, *40*, 2004-2021.
- (25) Link, A. J.; Tirrell, D. A. Cell surface labeling of Escherichia coli via copper(I)-catalyzed [3+2] cycloaddition. *J. Am. Chem. Soc.* **2003**, *125*, 11164-11165.
- (26) Bodine, K. D.; Gin, D. Y.; Gin, M. S. Synthesis of readily modifiable cyclodextrin analogues via cyclodimerization of an alkynyl-azido trisaccharide. *J. Am. Chem. Soc.* **2004**, *126*, 1638-1639.
- (27) Sawyer, T. K.; Sanfilippo, P. J.; Hruby, V. J.; Engel, M. H.; Heward, C. B.; Burnett, J. B.; Hadley, M. E. 4-Norleucine, 7-D-phenylalanine-alpha-melanocyte-stimulating hormone: a highly potent alpha-melanotropin with ultralong biological activity. *Proc. Natl. Acad. Sci. USA* **1980**, *77*, 5754-5758.
- (28) Haskell-Luevano C., Cone R. D., Monck E. K., Wan Y. P. Structure activity studies of the melanocortin-4 receptor by in vitro mutagenesis: identification of agouti-related protein (AGRP), melanocortin agonist and synthetic peptide antagonist interaction determinants. *Biochemistry* **2001**, *40*, 6164-6179.

- 1
2
3 (29) Chen, W.; Shields, T. S.; Stork, P. J. S.; Cone, R. D. A colorimetric assay for measuring
4 activation of Gs- and Gq-coupled signaling pathways. *Anal. Biochem.* **1995**, *226*, 349-354.
5
6
7
8
9 (30) Sun, H.; Greeley, D. N.; Chu, X. J.; Cheung, A.; Danho, W.; Swistok, J.; Wang, Y.; Zhao,
10 C.; Chen, L.; Fry, D. C. A predictive pharmacophore model of human melanocortin-4
11 receptor as derived from the solution structures of cyclic peptides. *Bioorg. Med. Chem.*
12 **2004**, *12*, 2671-2677.
13
14
15
16
17
18
19 (31) Mierke, D. F.; Kessler, H. Molecular-dynamics with dimethyl-sulfoxide as a solvent -
20 conformation of a cyclic hexapeptide. *J. Am. Chem. Soc.* **1991**, *113*, 9466-9470.
21
22
23
24
25 (32) Chatterjee, J.; Mierke, D.; Kessler, H. *N*-methylated cyclic pentaalanine peptides as
26 template structures. *J. Am. Chem. Soc.* **2006**, *128*, 15164-15172.
27
28
29
30
31 (33) Piantini, U.; Sorensen, O. W.; Ernst, R. R. Multiple quantum filters for elucidating NMR
32 coupling networks. *J. Am. Chem. Soc.* **1982**, *104*, 6800-6801.
33
34
35
36 (34) Bax, A.; Davis, D. G. Practical aspects of two-dimensional transverse NOE spectroscopy. *J.*
37 *Magn. Reson.* **1985**, *63*, 207-213.
38
39
40
41 (35) Jeener, J.; Meyer, B. H.; Bachman, P.; Ernst, R. R. Investigation of exchange processes by
42 two-dimensional NMR spectroscopy. *J. Chem. Phys.* **1979**, *71*, 4546-4553.
43
44
45
46 (36) Goddard, T. D.; Kneller, D. G.; SPARKY 3 NMR software. University of California, San
47 Francisco **2001**.
48
49
50
51
52 (37) Wüthrich, K. NMR of Proteins and Nucleic Acids. John Wiley & Sons: New York **1986**.
53
54
55
56
57
58
59
60

- 1
2
3
4
5
6
7
8
9
10
11
12
13
14
15
16
17
18
19
20
21
22
23
24
25
26
27
28
29
30
31
32
33
34
35
36
37
38
39
40
41
42
43
44
45
46
47
48
49
50
51
52
53
54
55
56
57
58
59
60
- (38) Hutchinson, E. G.; Thornton, J. M. PROMOTIF-a program to identify and analyze structural motifs in proteins. *Protein Sci.* **1996**, *5*, 212-220.
- (39) Sugg, E. E.; Castrucci, A. M.; Hadley, M. E.; van Binst, G.; Hruby, V. J. Cyclic lactam analogues of Ac-[Nle⁴]alpha-MSH4-11-NH₂. *Biochemistry* **1988**, *27*, 8181-8188.
- (40) Al-Obeidi, F.; O' Connor, S. D.; Job, C.; Hruby, V. J.; Pettitt, B. M. NMR and quenched molecular dynamics studies of superpotent linear and cyclic alpha-melanotropins. *J. Pept. Res.* **1998**, *51*, 420-431(41) Cho, M. K.; Lee, C. J.; Lee, C. H.; Li, S. Z.; Lim, S. K.; Baik, J. H.; Lee, W. Structure and function of the potent cyclic and linear melanocortin analogues. *J. Struct. Biol.* **2005**, *150*, 300-308.
- (42) Kaiser, E.; Colecott, R.; Bossinger, C.; Cook, P. Color test for detection of free terminal amino groups in the solid-phase synthesis of peptides. *Anal. Biochem.* **1970**, *34*, 595-598.
- (43) Xiang, Z.; Litherland, S. A.; Sorensen, N. B.; Proneth, B.; Wood, M. S.; Shaw, A. M.; Millard, W. J.; Haskell-Luevano, C. Pharmacological characterization of 40 human melanocortin-4 receptor polymorphisms with the endogenous proopiomelanocortin-derived agonists and the agouti-related protein (AGRP) antagonist. *Biochemistry* **2006**, *45*, 7277-7288.
- (44) Xiang, Z.; Pogozeva, I. D.; Sorenson, N. B.; Wilczynski, A. M.; Holder, J. R.; Litherland, S. A.; Millard, W. J.; Mosberg, H. I.; Haskell-Luevano, C. Peptide and small molecules rescue the functional activity and agonist potency of dysfunctional human melanocortin-4 receptor polymorphisms. *Biochemistry* **2007**, *46*, 8273-8287.

Table of Contents Graphic





50x28mm (300 x 300 DPI)